BIOCHEMISTRY
including biophysical chemistry & molecular biology
Article

Biochemistry **2010,** *49,* 2697–2704 2697
DOI: 10.1021/bi901875x

Binding of Adenosine-Based Ligands to the MjDim1 rRNA Methyltransferase: Implications for Reaction Mechanism and Drug Design[†,‡]

Heather C. O'Farrell,[§,∥] Faik N. Musayev,[∥,⊥] J. Neel Scarsdale,[∥,@] and Jason P. Rife*[,§,∥,@]

[§]*Department of Physiology and Biophysics,* [∥]*Institute for Structural Biology and Drug Design,* [⊥]*Department of Medicinal Chemistry, and* [@]*Department of Biochemistry, Virginia Commonwealth University, Richmond, Virginia 23298-0133*

Received November 2, 2009; Revised Manuscript Received February 15, 2010

ABSTRACT: The KsgA/Dim1 family of proteins is intimately involved in ribosome biogenesis in all organisms. These enzymes share the common function of dimethylating two adenosine residues near the 3′-OH end of the small subunit rRNA; orthologs in the three kingdoms, along with eukaryotic organelles, have evolved additional functions in rRNA processing, ribosome assembly, and, surprisingly, transcription in mitochondria. The methyltransferase reaction is intriguingly elaborate. The enzymes can bind to naked small subunit rRNA but cannot methylate their target bases until a subset of ribosomal proteins have bound and the nascent subunit has reached a certain level of maturity. Once this threshold is reached, the enzyme must stabilize two adenosines into the active site at separate times and two methyl groups must be transferred to each adenosine, with concomitant exchanges of the product *S*-adenosyl-L-homocysteine and the methyl donor substrate *S*-adenosyl-L-methionine. A detailed molecular understanding of this mechanism is currently lacking. Structural analysis of the interactions between the enzyme and substrate will aid in this understanding. Here we present the structure of KsgA from *Methanocaldococcus jannaschii* in complex with several ligands, including the first structure of *S*-adenosyl-L-methionine bound to a KsgA/Dim1 enzyme in a catalytically productive way. We also discuss the inability thus far to determine a structure of a target adenosine bound in its active site.

The Dim1/KsgA methyltransferases play important roles in ribosome biogenesis in all organisms (*1*). All members of this family share the common function of transferring four methyl groups from *S*-adenosyl-L-methionine (SAM)[1] to two adenosines of the small subunit rRNA. Details of the enzymatic mechanism have been slow to emerge and remain inadequate, in part because of the remarkable complexity of the reactions catalyzed. Four SAM molecules must sequentially bind to the active site and donate a methyl group, and the resultant *S*-adenosyl-L-homocysteine (SAH) molecule must be exchanged for the next SAM molecule. Similarly, two adenosines must each have separate access to the active site. In addition, the enzyme requires a mostly assembled small subunit in a specific conformation as a substrate (*2*, *3*), and the enzyme−subunit binding interaction is distal from the site of methylation (*4*). This mode of binding allows the protein to bind to nascent rRNA early in the maturation process but delay methylation until a more fully assembled particle is formed, bringing the target adenosines into the proximity of the active site.

In addition to their methyltransferase activity, KsgA/Dim1 proteins have further roles in ribosome biogenesis and other cellular functions. Eukaryotic Dim1 is an essential part of the processome, a large multifactor complex that is responsible for early processing and modification of the nascent 40S subunit. Knockout of Dim1 is lethal, leading to improper nucleolytic cleavage of the pre-rRNA (*5*, *6*). Dim1's enzymatic activity is not required for its role in rRNA processing; a catalytically inactive Dim1 can complement Dim1 knockout and support normal rRNA maturation (*7*). Bacterial KsgA is also important for ribosome biogenesis, although this function is distinct from Dim1's mode of action (*8*). Knockout of KsgA is not lethal under normal conditions but is deleterious at low temperatures, leading to accumulation of aberrant pre-30S subunit particles. Importantly, and in contrast to Dim1, KsgA's catalytic activity is a key component of this role. KsgA serves as a gatekeeper in the biogenesis pathway, and methylation of correctly formed pre-30S particles by KsgA allows release of the nascent subunit and final processing steps to occur. Also unlike the case for Dim1, overexpression of catalytically inactive KsgA is toxic at all temperatures.

To date, six members of this family have been described crystallographically, in apo and ligand-bound forms: KsgA from *Escherichia coli* (*9*) (EcKsgA), *Aquifex aeolicus* (*10*) (AaKsgA), and *Thermus thermophilus* (*11*) (TtKsgA) and Dim1 from *Plasmodium falciparum* (*12*) (PfDim1), *Homo sapiens* (A. Dong et al., structure published in the RCSB Protein Data Bank; HsDim1), and *Methanocaldococcus jannaschii* (*13*) (MjDim1). Figure 1 shows a sequence alignment of key regions of these six proteins. Structural analysis is aided by comparison with related methyltransferases. ErmC′ is a paralogous descendant of the KsgA/Dim1 lineage (*1*) that dimethylates a single adenosine in the 23S rRNA (*14*). This modification confers resistance to the MLS-B class of antibiotics (*15*). Although details of the catalytic

[†]This work was supported by National Institutes of Health Grant 5R01GM066900.

[‡]Atomic coordinates have been deposited into the Protein Data Bank as entries 3GRR (SAH), 3GRU (AMP), 3GRV (adenosine), and 3GRY (SAM).

*To whom correspondence should be addressed. Phone: (804) 828-7488. Fax: (804) 828-7382. E-mail: jason.rife@vcu.edu.

[1]Abbreviations: SAM, *S*-adenosyl-L-methionine; SAH, *S*-adenosyl-L-homocysteine; AMP, adenosine monophosphate; MLS-B, macrolide-lincosamide-streptogramin B; MTA, 5′-methylthioadenosine; rmsd, root-mean-square deviation.

Published on Web 02/17/2010

```
                  I              II             III            IV             VIII
MjDim1   33 VVLEIGLGKGILT  56 YVIEIDKSL   82 WGDALKVD  101 NLPYQISS  167 FYPKPAVYS
EcKsgA   40 AMVEIGPGLAALT  63 TVIELDRDL   89 QQDAMTFN  113 NLPYNIST  181 FTPPPKVDS
AaKsgA   33 TVLEVGGGTGNLT  57 YVIELDREM   81 NEDASKFP  101 NLPYNVAS  166 FVPPPKVQS
TtKsgA   49 PVFEVGPGLGALT  72 TAIEKDLRL   97 FQDALLYP  117 NLPYHIAT  184 FFPPPKVWS
HsDim1   59 VVLEVGPGTGNMT  82 VACELDPRL  111 VGDVLKTD  128 NLPYQISS  196 FRPPPKVES
PfDim1  101 IVLEIGCGTGNLT 124 ITIDIDSRM  152 EGDAIKTV  169 NIPYKISS  137 FNPPPKVDS
              :.*:* * . :*      ..:.*  :       *:.       *:** : :      * *.*.* *
```

FIGURE 1: Structure-based sequence alignment of key motifs of KsgA/Dim1 proteins. Roman numerals indicate conserved structural motifs. Conservation is indicated below each residue; an asterisk designates absolutely conserved residues, a colon highly conserved residues, and a period residues that are conserved in four of the five proteins. Residues colored red make direct contact with SAM in the MjDim1 crystal structure. Accession numbers are NP_248023 (Mj), P06992 (Ec), NP_214246 (Aa), YP_143349 (Tt), NP_055288 (Hs), and XP_001348329 (Pf).

mechanism have diverged, the two enzyme families share a high degree of sequence and structural homology. The crystal structure of ErmC′ has been determined in the unliganded form (*16*), as well as in complex with the substrate SAM, the product SAH, and the inhibitor analogue sinefungin (*17*). The DNA adenosine methyltransferases are less homologous to KsgA/Dim1, but structural comparison can still be instructive. These enzymes transfer a single methyl group to a single deoxyadenosine in chromosomal DNA; the identity of the DNA target sequence depends on the specific enzyme. M.TaqI is a representative of this family of enzymes; the structure of this enzyme has been determined in complex with a variety of ligands (*18*−*22*) (T. Lenz et al., structure published in the RCSB Protein Data Bank), including ternary complexes with a SAM analogue, duplex DNA, and the target adenosine flipped into position in the active site.

Antibiotic resistance is a growing problem worldwide (*23*). Diseases once thought to have been essentially overcome in developed countries are emerging as new threats that are increasingly difficult to treat with current antibacterial drugs. Comartin and Brown recently proposed that ribosome assembly factors should be considered as important targets for new antibiotics (*24*), and Champney suggested that inhibition of the ribosome biogenesis process could be an important direction for drug design (*25*). KsgA would seem to be an ideal candidate for antibiotic research. This protein is universally conserved in bacteria and has been characterized structurally, and as mentioned above, catalytic inactivation of KsgA has a profoundly deleterious effect on ribosome assembly and cell survival (*8*).

A structural understanding of ligand binding to the KsgA/Dim1 active site is the first step in developing this factor as a drug target. Enzyme−ligand structures will also be valuable for a better understanding of the complex mechanism of this protein family. Early biochemical data suggested that EcKsgA does not bind SAM efficiently in the absence of 30S subunits (*26*); whether this is true for other members of the family remains an open question. The crystal structure of HsDim1 includes a bound SAM molecule; however, comparison to other SAM-dependent methyltransferases suggests that this mode of binding is not catalytically productive. We previously described high-resolution crystal structures of EcKsgA (*9*) and MjDim1 (*13*). Here, we report structures of MjDim1 in complex with the substrate molecules and analogues SAM, SAH, adenosine, and AMP. Our results highlight important features of substrate binding and form a foundation for further analysis. Details of enzyme−ligand binding presented here will be valuable in the rational design and optimization of antibacterial drug candidates.

MATERIALS AND METHODS

Protein Purification and Crystallography. MjDim1 containing the K137A and E138A mutations was used for crystallography, as this form generated highly diffracting crystals in a previous study (*13*). Mutagenesis of this and other mutants was performed using the Stratagene QuikChange Kit according to the manufacturer's protocol. The resulting plasmids were transformed into *E. coli* XL1-Blue cells, and mutants were confirmed by sequencing. Protein expression and purification were conducted as previously described (*27*). Protein purity was assessed by SDS−PAGE. Crystals of the apo form of MjDim1 were obtained as previously described (*13*).

We produced binary complexes of MjDim1 with adenosine, AMP, SAM, and SAH by soaking unliganded crystals in 10, 25, 2.5, and 10 mM corresponding ligand solutions, respectively, at 17 °C for 8−24 h. Protein crystals were placed in a 5 μL hanging drop containing 38 mM NaMES (pH 6.2), 25% PEG 8000, 4 mM $MgCl_2$, 6 mM NH_4Cl, 75 mM $(NH_4)_2SO_4$, 25 mM Tris-HCl, and the corresponding ligands and equilibrated against reservoir solution containing 30−35% PEG 8000. For X-ray data collection, crystals were soaked for a few seconds in 5−6 μL of reservoir solution with appropriate ligands, before being flash-cooled in a liquid nitrogen stream. X-ray data were collected at 100 K with a Molecular Structure Corp. (MSC) X-Stream Cryogenic Crystal Cooler System and an R-Axis IV^{++} image plate detector with a Rigaku MicroMax-007 X-ray source equipped with MSC Varimax confocal optics operating at 40 kV and 20 mA. Data were processed and scaled with D*TREK. Data collection and refinement statistics are listed in Table 1.

Initial models for each complex were obtained by rigid body refinement of the coordinates of MjDim1 from Protein Data Bank (PDB) entry 3FYD (*13*). All models were subjected to one cycle of Cartesian simulated annealing in PHENIX (*28*) version 1.3 followed by alternating cycles of manual rebuilding in COOT (*29*) using $2mF_o - dF_c$ and $mF_o - dF_c$ maps and computational maximum likelihood refinement with REFMAC version 5.2.0019 (*30*). Figures were generated using Pymol (*31*).

Activity Assay. The in vitro activity assay was performed as previously described (*27*). Assays contained 0.2 μM unmethylated 30S subunits, 0.2 μM enzyme, and 20 μM [^{3}H-*methyl*]SAM (780 cpm/pmol) in 40 mM Tris (pH 7.4), 40 mM NH_4Cl, 4 mM $MgCl_2$, and 6 mM β-mercaptoethanol. Reaction mixtures were incubated at 37 °C for 2 h, deposited onto DE-81 filters, washed twice with ice-cold 5% TCA, and rinsed briefly with ice-cold ethanol. Filters were air-dried and counted.

RESULTS

Structural Overview. Crystals of the well-diffracting K137A/E138A mutant of MjDim1 were grown as previously described (*13*) and were soaked with the ligands SAM, SAH, adenosine, and AMP. The resultant cocrystals all belonged to the $P2_1$ space group and contained one copy of the protein per asymmetric unit (Table 1). Density was seen for residues 10−272, except in the case of the MjDim1−adenosine complex, which did

Table 1: X-ray Data Collection and Refinement

	SAH	AMP	ADN	SAM
Data Collection				
space group	$P2_1$	$P2_1$	$P2_1$	$P2_1$
unit cell parameters				
a (Å)	40.38	40.53	40.26	40.47
b (Å)	66.3	66.28	66.02	67.02
c (Å)	62.06	62.01	61.69	62.15
β (deg)	107.76	107.52	108.35	107.85
overall resolution (Å) (high-resolution shell)	17.70−1.80 (1.86−1.80)	38.65−1.60 (1.66−1.60)	22.01−1.90 (1.97−1.90)	22.34−2.20 (2.28−2.20)
no. of observations	27022 (2550)	39244 (2542)	22955 (2323)	14252 (1382)
completeness (%)	93.3 (88.5)	94.8 (61.6)	94.5 (96.4)	88.0 (85.0)
R_{merge}	0.038 (0.347)	0.035 (0.293)	0.052 (0.326)	0.08 (0.363)
$I/\sigma(I)$	18.7 (4.0)	27.2 (4.6)	19.5 (4.5)	14.0 (3.0)
multiplicity	4.59 (4.45)	7.00 (5.15)	6.34 (6.39)	6.18 (6.07)
Wilson plot B (Å^2)	40.5	34.52	49.3	56.2
optical resolution (Å)	1.55	1.4	1.59	1.78
Refinement				
overall resolution range (Å) (high-resolution shell)	17.50−1.80 (1.846−1.80)	22.00−1.60 (1.641−1.60)	22.00−1.90 (1.949−1.90)	32.00−2.20 (2.26−2.20)
no. of reflections in the working/free set	24273/2733	35290/3921	21776/1164	12810/1431
no. of protein atoms	2116	2136	2118	2114
no. of water atoms	218	346	221	125
R_{work} overall (high-resolution shell)	0.182 (0.285)	0.180 (0.258)	0.180 (0.220)	0.237 (0.304)
R_{free} overall (high-resolution shell)	0.234 (0.332)	0.212 (0.292)	0.240 (0.310)	0.295 (0.331)
$R_{overall}$	0.187	0.184	0.183	0.243
$\langle B \rangle$ (Å^2)	45.2	41.2	48	53.4
Cruickshank's DPI (Å)	0.127	0.088	0.149	0.27
estimated maximal coordinate error	0.113	0.081	0.123	0.214
rmsd for bond lengths (Å)	0.009	0.009	0.009	0.009
rmsd for bond angles (deg)	1.123	1.139	1.11	1.139
Ramachandran plot				
most favored (%)	93.9	95.5	94.7	93.1
additionally allowed (%)	6.1	4.5	4.9	6.5
generously allowed (%)			0.4	0.4
forbidden (%)				

not show density for residue 272. The MjDim1−SAM complex diffracted to a resolution of 2.2 Å and contained 125 water molecules. The MjDim1−SAH complex diffracted to a resolution of 1.8 Å and contained 218 water molecules. The MjDim1−adenosine complex diffracted to a resolution of 1.9 Å and contained 221 water molecules. The MjDim1−AMP complex diffracted to a resolution of 1.6 Å and contained 346 water molecules. Each structure contained only one ligand molecule; in each case, the electron density corresponding to the ligand was strong and clearly allowed for the unambiguous placement of the ligands. Figure 2 shows the electron density for each of the four ligands.

Ligand−Enzyme Interactions. The structure of MjDim, like other related enzymes, contains a negatively charged pocket in the active site (Figure 3A); as seen in the structures of other methyltransferases, SAM bound in this pocket. The ligand is stabilized by a variety of hydrogen bonding and van der Waals interactions (Figure 3B). N6 of the adenosine moiety makes a hydrogen bond to D84, and N1 of the adenine ring is in hydrogen bond contact with the peptide backbone, interacting with the amide nitrogen of A85. The adenine is also bracketed by van der Waals interactions with residues I60 and P103. E59 has a bifurcated hydrogen bonding interaction with the two hydroxyl groups of the ribose. Additionally, the 3′-OH of the ribose makes a hydrogen bond with the backbone nitrogen of G40. The carboxyl group of the methionine moiety makes a hydrogen

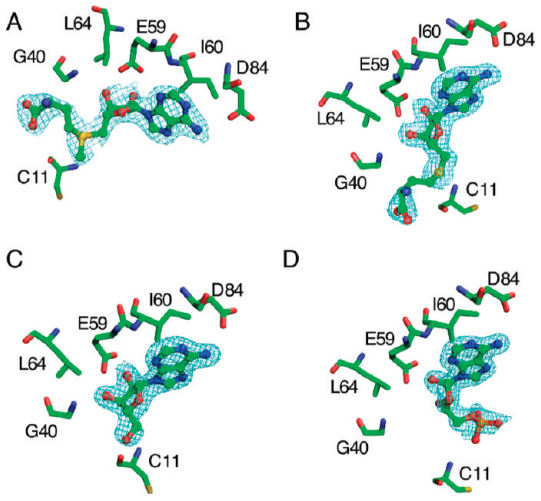

FIGURE 2: $2mF_o - dF_c$ electron density map of ligands contoured at 1σ. Amino acid side chains that are in the proximity of the ligands are labeled: (A) SAM, (B) SAH, (C) adenosine, and (D) AMP.

bond to the amide nitrogen of residue N101 as well as contacts to the backbone amide of L13, while the amine group makes hydrogen bond contacts to the side chain of E36 and the backbone carbonyl of G38. This positioning orients the methyl group downward toward the target adenosine binding pocket. With the exception of A85 and I60, these residues are among the

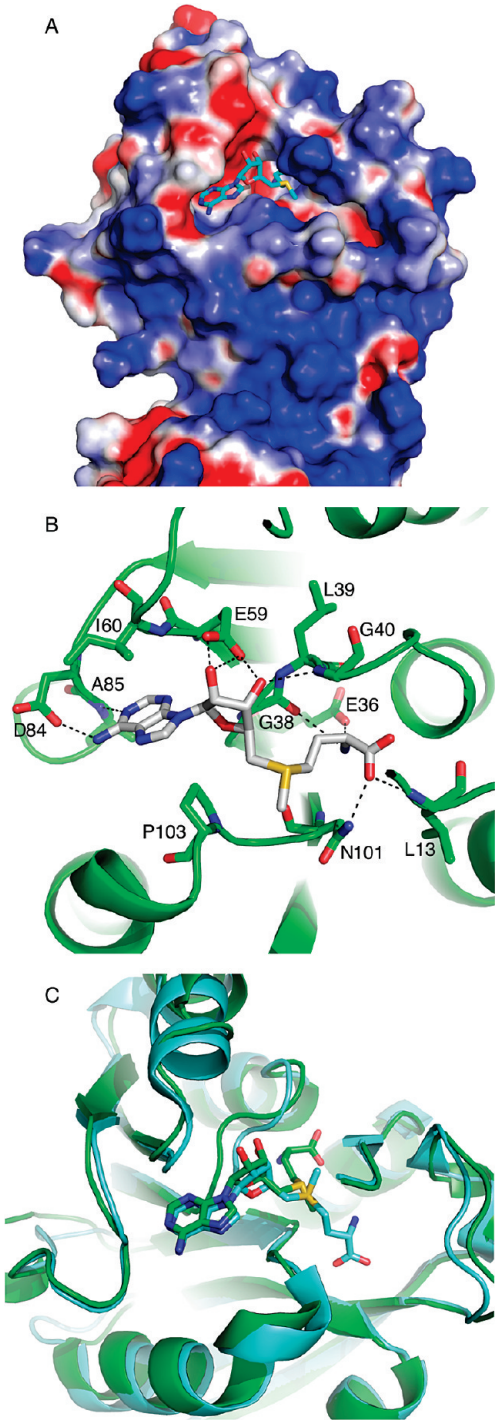

FIGURE 3: SAM binding. (A) Charge distribution of the active site surface of MjDim1. Red indicates negative charge, and blue indicates positive charge. SAM is shown as a stick representation in the active site. (B) Interaction of SAM with active site residues of MjDim1. Residues that interact with SAM are shown in stick representation and labeled. Dashes indicate hydrogen bonding interactions. (C) Binding mode of SAM in MjDim1 (green) compared to HsDim1 (PDB entry 1ZQ9; A. Dong et al., structure published in the RCSB Protein Data Bank; cyan).

most conserved in the KsgA/Dim1 family (*32*); A85 and I60 are not strictly conserved, but these two residues are generally found to be hydrophobic.

Comparison of the MjDim1−SAM structure with the HsDim1−SAM structure shows very different binding modes for the ligand (Figure 3C). The adenosine moiety binds similarly, but the methionine of SAM bound to HsDim1 is rotated about the C5′−S bond by approximately 110° as compared to the MjDim1 structure. This results in the methionine moiety extending downward into and blocking the target adenosine pocket, with the methyl group oriented away from where the target base is predicted to bind.

In the protein conformation found in the crystal structure, MjDim1 is clearly able to bind SAM. In contrast, previous evidence suggests that EcKsgA is not able to bind SAM appreciably (*26*), despite having an apparently preformed SAM binding site (*9*). To investigate this apparent disparity, we compared the EcKsgA and MjDim1 binding sites by rendering a van der Waals surface of each protein. As seen in Figure 4, the EcKsgA binding site narrows around the methionine binding area, as compared to MjDim1. The larger binding pocket seen in the MjDim1 structure appears to be intrinsic to the protein and not a result of ligand binding, as the unliganded structure has a similarly sized pocket (*13*). Interestingly, the HsDim1 structure shows a narrowing of the binding pocket similar to that of EcKsgA.

The catalytic product SAH binds to MjDim1 in essentially the same way as SAM, making the same hydrogen bonding and nonpolar contacts (not shown). The mode of binding of both ligands to MjDim1 closely resembles the interactions of AaKsgA and TtKsgA with the ligands SAH and 5′-methylthioadenosine (MTA), respectively (Figure 5). The ligands interact with essentially the same set of protein residues and are oriented the same way, the exception being that the methionine moiety of SAH bound to AaKsgA has a slightly different trajectory between the β- and γ-carbon atoms as compared to the SAM and SAH molecules bound to MjDim1.

To improve our understanding of the mode of binding of the target base to the active site, we soaked adenosine into MjDim1 crystals. However, even at high concentrations of adenosine (up to 10 mM), we did not observe any electron density in the target site. This strongly suggests that there was no appreciable binding of adenosine to the target adenosine pocket. Instead, adenosine bound in the SAM pocket in a manner analogous to that of the adenosine moiety of SAM (Figure 6). In a further effort to define the enzyme−target binding interaction, we soaked AMP into MjDim1 crystals. We predicted that the bulky, highly charged phosphate group of the AMP molecule would preclude the binding interaction seen with the adenosine ligand. Surprisingly, AMP also bound in the SAM pocket rather than the adenosine pocket, albeit with a binding mode slightly different from that of the previously discussed ligands (Figure 6). The adenine base bound in a manner similar to those of SAM, SAH, and adenosine, with a hydrogen bond interaction between D84 and N6. However, the presence of a phosphate group causes the ribose to rotate around the χ bond as compared to SAM. The 2′-OH of the ribose is still in position to form a hydrogen bond to E59; the 3′-OH has moved away from E59, and its interaction with that residue is now mediated by a water molecule that is located in approximately the same position as the 3′-OH of the other ligands. The phosphate group is oriented toward the target adenosine pocket and does not appear to directly interact with the protein.

Mutagenesis of E. coli KsgA. We previously made use of an alanine mutation of E66 in EcKsgA, equivalent to E59 in MjDim1, that abrogated in vivo methyltransferase activity as determined by primer extension (*8*). We performed in vitro activity assays with the E66A mutant and the D91A mutant

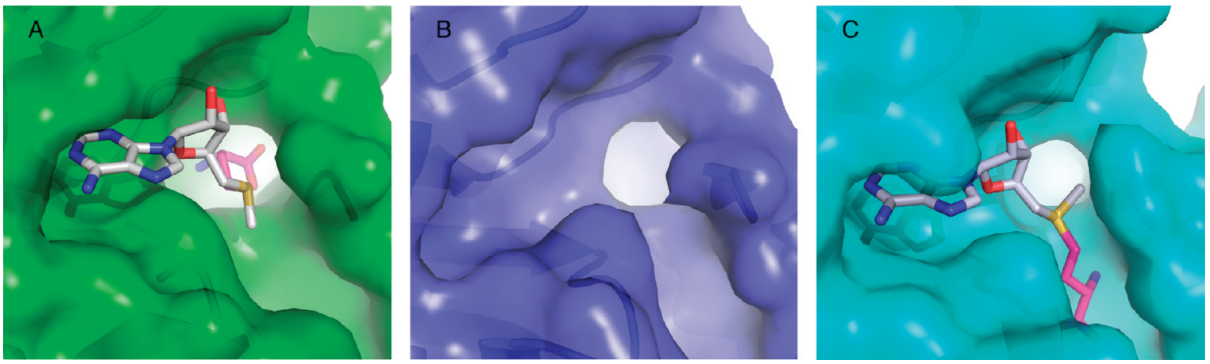

FIGURE 4: Comparison of van der Waals surface of SAM binding pockets. (A) MjDim1 surface, (B) EcKsgA surface [PDB entry 1QYR (*9*)], and (C) HsDim1 surface.

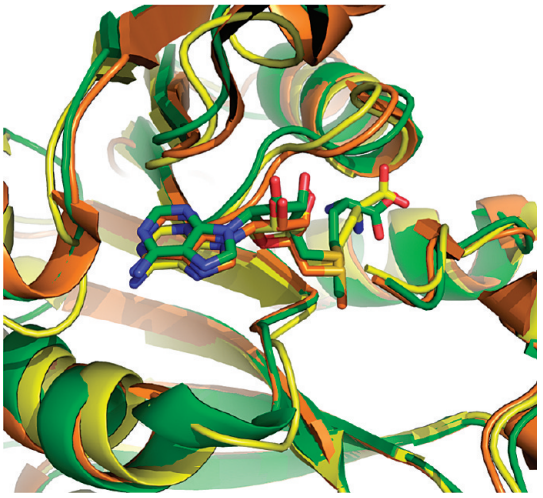

FIGURE 5: SAH and other ligand binding. Active sites of MjDim1 with SAH (green), AaKsgA with SAH [PDB entry 3FTF (*10*), yellow], and TtKsgA with MTA [PDB entry 3FUW (*11*), orange].

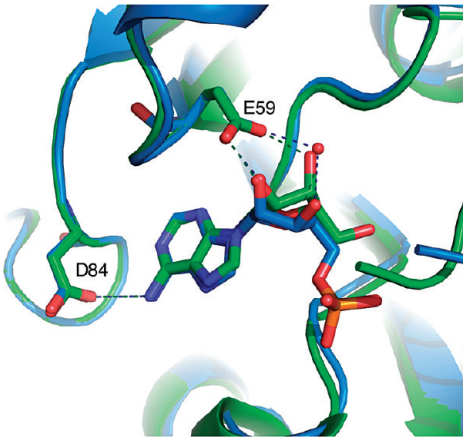

FIGURE 6: Binding of adenosine (green) and AMP (blue) to MjDim1. Dashes indicate hydrogen bonds.

(D84 in MjDim1) and showed that either mutation renders the enzyme catalytically inactive (Figure 7).

Two aromatic residues have been suggested to stabilize the target adenosine into the active site for catalysis. The first is part of the highly conserved motif IV and corresponds to Y104 of MjDim1; the second is part of motif VIII, F167 in MjDim1. We tested the importance of these residues with respect to enzymatic activity by mutagenesis of the corresponding residues, Y116 and

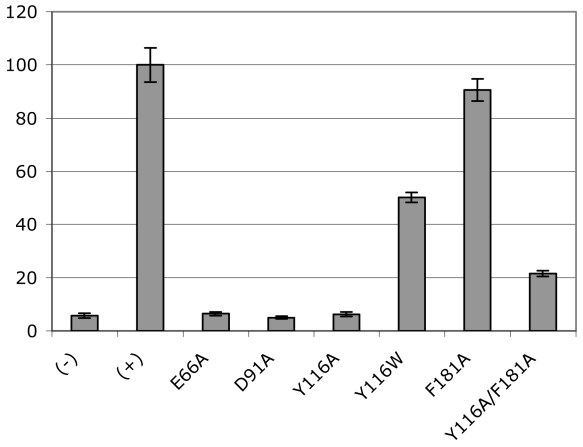

FIGURE 7: Mutagenic analysis of the active site. The negative control, indicated by (−), contained no enzyme. The positive control, indicated by (+), contained the wild-type enzyme. The in vitro activity of the mutant proteins was normalized to the positive control and is presented as a percentage of wild-type activity.

F181, in EcKsgA (Figure 7). The F181A mutant has activity comparable to that of the wild-type enzyme. The EcKsgA Y116A mutation, on the other hand, abolished activity in the in vitro assay, while the more conservative Y116W substitution retained some activity. The Y116A/F181A double mutant, while only ~20% as active as the wild type, shows activity significantly higher than that of the Y116A single mutant.

DISCUSSION

Binding of SAM Analogues. Several groups have attempted to determine the structure of KsgA/Dim1 with the SAM substrate bound in the active site, with limited success. The structure of HsDim1 was determined with a bound SAM molecule (A. Dong et al., structure published in the RCSB Protein Data Bank); however, the binding mode probably does not reflect the catalytically relevant conformation (see below). More recently, attempts have been made to determine the structures of *T. thermophilus* KsgA (TtKsgA) and *A. aeolicus* KsgA (AaKsgA) in complex with SAM. In the first case, the crystallographic conditions led to degradation of the SAM molecule, and the resulting structure contained the breakdown product 5′-methylthioadenosine rather than the intact SAM structure (*11*). In the case of AaKsgA, the crystal structure contained SAH rather than SAM, for reasons that are not clear (*10*). To improve our understanding of the enzyme−ligand interaction, we soaked SAM, as well as the product SAH, into MjDim1 crystals. Both molecules

bound in the predicted SAM-binding pocket and interacted with conserved residues that are found in canonical motifs of SAM-dependent methyltransferases, most notably, E59 in motif II and D84 in motif III. Mutation of either of these residues in EcKsgA resulted in the loss of any measurable enzymatic activity.

Poldermans et al. showed that SAM binding to free EcKsgA is weak and suggested an ordered binding mechanism whereby KsgA binding to 30S subsequently allows SAM binding (*26*). More recently, Tu et al. observed that AaKsgA crystallized with a ligand in the active site only if the protein was also bound to RNA (*10*). The authors suggested that RNA binding stabilizes the protein in a conformation that allows subsequent ligand binding. However, upon purification of MjDim1, we observed that the protein showed a strong absorbance peak at 260 nm (data not shown), suggesting the presence of bound nucleic acid, or possibly SAM. The MjDim1−SAM structure indicates that under the conditions used here MjDim1, unlike EcKsgA, is able to bind SAM in the absence of 30S subunits. We earlier observed differences in mechanism between EcKsgA and MjDim1 activity under certain conditions (*27*). It is possible that the differential ability of the free enzyme to bind SAM may have implications for differences in the mechanistic details.

Closer examination of the active sites for the two enzymes reveals an intriguing variance. In Figure 4, we aligned the structures of EcKsgA and the HsDim1−SAM complex onto the MjDim1−SAM structure. When each structure is rendered with a van der Waals surface representation, MjDim1 displays a pocket that surrounds the methionine moiety of SAM. In EcKsgA, this pocket is distinctly narrower. The shape of this pocket reflects the trajectory of motif I, termed the G-loop; this motif is a hallmark of SAM-dependent methyltransferases. The consensus sequence for this motif in KsgA/Dim1 proteins is E-I/V-G-**P**-G and in EcKsgA is E-I-G-**P**-G. However, the MjDim1 sequence is E-I-G-**L**-G. The identity of the fourth residue in this sequence, either a P or an L, may be related to the shape of the binding pocket and thus determine the ability of the free enzyme to bind SAM.

Strikingly, HsDim1 contains the sequence E-V-G-**P**-G, and its methionine binding pocket is also much smaller than that of Mj-Dim1. Comparison of the MjDim−SAM and HsDim1−SAM structures with previously published data highlights that the SAM is bound to HsDim1 in a catalytically unproductive way (Figure 3C). A molecular modeling study of the M.TaqI DNA methyltransferse found that catalysis is due to the proper positioning of the two substrates with respect to each other so that the amine group of the adenosine can carry out a nucleophilic attack on the methyl group of the SAM (*33*). In a ternary structure of M.TaqI in complex with DNA and a SAM analogue, the target adenosine is positioned in the active site so that the amine group forms hydrogen bonds with the carboxyl group of residue N105 and the backbone carbonyl of P106 (*20*). In this orientation, the amine group, the methyl group, and the sulfur atom will be at the correct distance and angle to achieve the modeled transition state geometry and facilitate transfer of the methyl group. In the MjDim1−SAM structure, the methyl group is positioned essentially as in the M.TaqI−SAM crystal structure with respect to these two active site residues, N101 and L102 in MjDim1. Therefore, we believe that this structure represents a binding mode that is competent for methyl transfer. In this orientation, the methionine moiety of SAM is extended along the active site, with the methyl group to be transferred oriented toward the target adenosine pocket. In the HsDim1 structure, the methionine moiety turns downward and occludes the target adenosine-binding site; the methyl group to be transferred is oriented toward the interior of the protein. It is possible that the narrower binding pocket does not allow proper binding of the SAM ligand and forces it into a conformation that is not catalytically relevant.

AaKsgA contains the sequence E-V-G-**G**-G. This enzyme was shown to bind SAH in a ternary complex with RNA; however, the mode of binding of the ligand is slightly different from that of SAH bound to MjDim1. The adenosine portion of the SAH molecule binds in a similar manner, although the 3′-hydroxyl has moved away from the side chain of the motif II Glu residue (E60 in AaKsgA) and is outside of hydrogen bonding range. The sulfur atom is positioned in a manner analogous to that of the same ligand in MjDim1, but the remainder of the methionine moiety takes a slightly different trajectory that results in a relative rotation of the carbonyl and amine groups. It is perhaps notable that the AaKsgA−SAH−RNA structure was obtained in drops that contained SAM, but the SAM ligand was apparently unable to bind to the enzyme, at least under the conditions used for crystallography.

Clearly, the mechanism of SAM binding and the specifics of SAM−SAH exchange remain unresolved at this time. The structure of MjDim1 in complex with SAM presented here represents the first such complex for this family of enzymes in which the substrate molecule appears to be correctly positioned for catalysis. Careful examination of this and related structures may provide clues to help guide further research on mechanistic details of the complex, multistep reaction catalyzed by the KsgA/Dim1 family of enzymes.

Binding of Adenosine Analogues. It was previously reported that adenosine acts as an inhibitor of the methyltransferase reaction, and the authors of that study proposed that the inhibition was via binding in the SAM pocket, rather than in the target adenosine pocket (*26*). Our cocrystal structure, showing adenosine bound in the SAM site, lends support to this hypothesis. In a further attempt to clarify the binding of the target adenosine, we soaked AMP into MjDim1 crystals with the prediction that the phosphate moiety would prevent binding to the SAM-binding site. To our surprise, the AMP molecule was still found in the SAM pocket, although the binding interactions of the adenosine moiety were distorted relative to the other ligands, presumably to accommodate the phosphate group.

These results taken together suggest that adenosine does not bind strongly to its binding pocket in the absence of the 30S substrate particle. The structure of M.TaqI has been determined in a ternary complex with a SAM analogue and a double-stranded DNA, with the target adenosine flipped out of the DNA helix and into the active site (*20*). This adenosine conformation is stabilized by two highly conserved aromatic residues. A tyrosine residue found in motif IV is seen to stack with the adenosine in a face-to-face interaction, while a phenylalanine in motif VIII provides an edge-to-face stacking interaction. Mutagenic analysis of these two residues in M.TaqI confirmed their importance for enzymatic activity (*34*). Kinetic and binding data led the authors to propose a role for the phenylalanine in flipping the target adenosine into the active site, with the tyrosine being required for proper catalytic positioning of the adenosine. To understand the roles, if any, these residues play in KsgA/Dim1 activity, we performed mutagenic analysis of the EcKsgA protein.

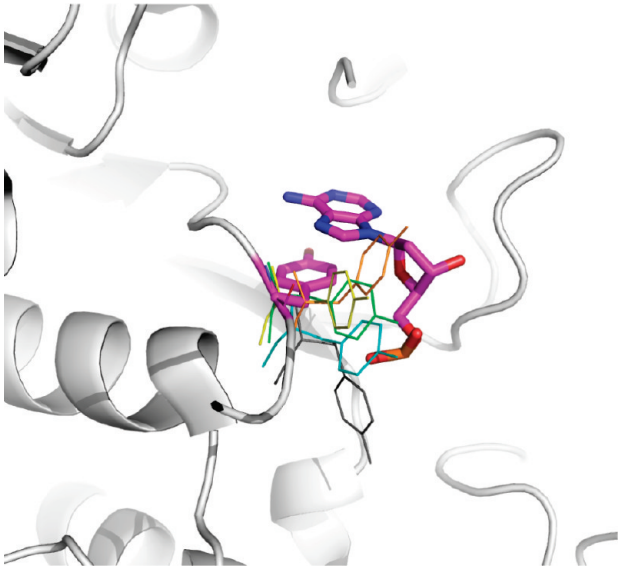

FIGURE 8: Tyrosine side chains of adenosine methyltransferases. M.TaqI [PDB entry 1G38 (*20*)] is colored white, with the tyrosine side chain and the target adenosine colored magenta. The tyrosine residue of MjDim1 is colored green, HsDim1 cyan, AaKsgA orange, TtKsgA yellow, and PfDim1 [PDB entry 2H1R (*12*)] gray. EcKsga is not included because this residue did not exhibit side chain density.

Mutation of the Y116 residue in motif IV to alanine resulted in a protein with no measurable activity. The more conservative Y116W mutation was tolerated, but this mutant still exhibited greatly reduced activity. Clearly, this residue is critically important to enzyme function, probably in binding and/or orienting the target base. Strikingly, in all of the KsgA/Dim1 structures, this residue either does not show side chain density, suggesting that it is disordered in the crystal, or has density but is pointing away from the active site (Figure 8). This may indicate that binding of the protein to 30S subunits is necessary to achieve the correct orientation of the tyrosine residue, which then allows the target adenosine to be stabilized in the binding pocket in an induced fit mechanism.

Mutation of the motif VIII phenylalanine, F181, to alanine in EcKsgA had no measurable effect on enzyme activity. This is in contrast to the results in M.TaqI (*34*). In addition, the equivalent mutation in ErmC′ (*35*) resulted in an enzyme with greatly reduced activity. Unlike the Erm enzymes and DNA methyltransferases, KsgA must separately accommodate two adenosines into the active site. The observed differences in mutant enzyme activity may reflect this requirement to exchange one adenosine for the other. Although this possibility is speculative, it is clear that this residue does not have the same importance in adenosine binding in the three groups. Curiously, adding the F181A mutation to the Y116A protein resulted in an increase in activity as compared to the Y116A single mutant. One hypothesis is that F181 provides an interaction with the target adenosine that is weak compared with the strong stacking interaction with Y116. In the presence of Y116, the lack of the phenylalanine ring has little effect on the enzyme's activity, as seen in the mutagenesis data. However, in the absence of Y116, F181 actually hinders the protein's enzymatic activity, possibly by stabilizing the target adenosine in a noncatalytic conformation. Removing both aromatic side chains restores the ability of the adenosine to sample the active site and be methylated, albeit at a much lower level than in the wild-type enzyme.

Implications for Drug Design. Catalytic inactivation of bacterial KsgA may prove to be an important strategy in the search for new antibacterial drugs. The enzyme−ligand structures presented here will be important starting points for rational drug design. We have highlighted specific interactions between residues in the active site and the SAM substrate and analogues. Interactions with E59 and D84 seem to be especially important. Interaction of SAM with only one of these residues is insufficient to allow enzymatic activity, as shown by mutagenic analysis. Our data also suggest that the target adenosine-binding pocket may not be a good candidate for potential adenosine-based inhibitors, although adenosine analogues have the potential to bind in the SAM pocket.

In a review of SAM-dependent methyltransferases, Schubert et al. performed a structural comparison of enzymes that are structurally related to KsgA/Dim1 (*36*). These enzymes methylate a variety of targets and are structurally divergent outside of the more conserved methyltransferase core but show a remarkable similarity in binding of the SAM or SAH molecule. Therefore, selectivity must be a concern in the design of KsgA/Dim1 inhibitors. Here, analysis of the HsDim1−SAM structure is particularly instructive, suggesting an intriguing mode of binding that could perhaps be exploited. The orientation of the methionine moiety could guide the design of ligands that build into the adenosine pocket from the SAM pocket. An inhibitor that bridges the active site and blocks both substrate-binding pockets could be a viable drug candidate. We believe that this strategy could help increase drug selectivity and reduce the likelihood of nonselective inhibition of other SAM-binding proteins.

REFERENCES

1. Rife, J. P. (2009) Roles of the Ultra-Conserved Ribosomal RNA Methyltransferase KsgA in Ribosome Biogenesis. In DNA and RNA Modification Enzymes: Structure, Mechanism, Function and Evolution (Grosjean, H., Ed.) 1st ed., pp 509−523, Landes Bioscience, Austin, TX.
2. Thammana, P., and Held, W. A. (1974) Methylation of 16S RNA during ribosome assembly in vitro. *Nature 251*, 682–686.
3. Desai, P. M., and Rife, J. P. (2006) The adenosine dimethyltransferase KsgA recognizes a specific conformational state of the 30S ribosomal subunit. *Arch. Biochem. Biophys. 449*, 57–63.
4. Xu, Z., O'Farrell, H. C., Rife, J. P., and Culver, G. M. (2008) A conserved rRNA methyltransferase regulates ribosome biogenesis. *Nat. Struct. Mol. Biol. 15*, 534–536.
5. Lafontaine, D., Delcour, J., Glasser, A. L., Desgres, J., and Vandenhaute, J. (1994) The DIM1 gene responsible for the conserved m6(2)Am6(2)A dimethylation in the 3′-terminal loop of 18 S rRNA is essential in yeast. *J. Mol. Biol. 241*, 492–497.
6. Lafontaine, D., Vandenhaute, J., and Tollervey, D. (1995) The 18S rRNA dimethylase Dim1p is required for pre-ribosomal RNA processing in yeast. *Genes Dev. 9*, 2470–2481.
7. Lafontaine, D. L., Preiss, T., and Tollervey, D. (1998) Yeast 18S rRNA dimethylase Dim1p: A quality control mechanism in ribosome synthesis? *Mol. Cell. Biol. 18*, 2360–2370.
8. Connolly, K., Rife, J. P., and Culver, G. (2008) Mechanistic insight into the ribosome biogenesis functions of the ancient protein KsgA. *Mol. Microbiol. 70*, 1062–1075.
9. O'Farrell, H. C., Scarsdale, J. N., and Rife, J. P. (2004) Crystal structure of KsgA, a universally conserved rRNA adenine dimethyltransferase in *Escherichia coli*. *J. Mol. Biol. 339*, 337–353.
10. Tu, C., Tropea, J. E., Austin, B. P., Court, D. L., Waugh, D. S., and Ji, X. (2009) Structural basis for binding of RNA and cofactor by a KsgA methyltransferase. *Structure 17*, 374–385.
11. Demirci, H., Belardinelli, R., Seri, E., Gregory, S. T., Gualerzi, C., Dahlberg, A. E., and Jogl, G. (2009) Structural rearrangements in the active site of the *Thermus thermophilus* 16S rRNA methyltransferase KsgA in a binary complex with 5′-methylthioadenosine. *J. Mol. Biol. 388*, 271–282.
12. Vedadi, M., Lew, J., Artz, J., Amani, M., Zhao, Y., Dong, A., Wasney, G. A., Gao, M., Hills, T., Brokx, S., Qiu, W., Sharma, S.,

Diassiti, A., Alam, Z., Melone, M., Mulichak, A., Wernimont, A., Bray, J., Loppnau, P., Plotnikova, O., Newberry, K., Sundararajan, E., Houston, S., Walker, J., Tempel, W., Bochkarev, A., Kozieradzki, I., Edwards, A., Arrowsmith, C., Roos, D., Kain, K., and Hui, R. (2007) Genome-scale protein expression and structural biology of *Plasmodium falciparum* and related apicomplexan organisms. *Mol. Biochem. Parasitol. 151*, 100–110.

13. Pulicherla, N., Pogorzala, L. A., Xu, Z. O., Farrell, H. C., Musayev, F. N., Scarsdale, J. N., Sia, E. A., Culver, G. M., and Rife, J. P. (2009) Structural and functional divergence within the Dim1/KsgA family of rRNA methyltransferases. *J. Mol. Biol. 391*, 884–893.
14. Zhong, P., Pratt, S. D., Edalji, R. P., Walter, K. A., Holzman, T. F., Shivakumar, A. G., and Katz, L. (1995) Substrate requirements for ErmC′ methyltransferase activity. *J. Bacteriol. 177*, 4327–4332.
15. Weisblum, B. (1995) Erythromycin resistance by ribosome modification. *Antimicrob. Agents Chemother. 39*, 577–585.
16. Bussiere, D. E., Muchmore, S. W., Dealwis, C. G., Schluckebier, G., Nienaber, V. L., Edalji, R. P., Walter, K. A., Ladror, U. S., Holzman, T. F., and Abad-Zapatero, C. (1998) Crystal structure of ErmC′, an rRNA methyltransferase which mediates antibiotic resistance in bacteria. *Biochemistry 37*, 7103–7112.
17. Schluckebier, G., Zhong, P., Stewart, K. D., Kavanaugh, T. J., and Abad-Zapatero, C. (1999) The 2.2 Å structure of the rRNA methyltransferase ErmC′ and its complexes with cofactor and cofactor analogs: Implications for the reaction mechanism. *J. Mol. Biol. 289*, 277–291.
18. Labahn, J., Granzin, J., Schluckebier, G., Robinson, D. P., Jack, W. E., Schildkraut, I., and Saenger, W. (1994) Three-dimensional structure of the adenine-specific DNA methyltransferase M.taqI in complex with the cofactor S-adenosylmethionine. *Proc. Natl. Acad. Sci. U.S.A. 91*, 10957–10961.
19. Schluckebier, G., Kozak, M., Bleimling, N., Weinhold, E., and Saenger, W. (1997) Differential binding of S-adenosylmethionine S-adenosylhomocysteine and sinefungin to the adenine-specific DNA methyltransferase M.TaqI. *J. Mol. Biol. 265*, 56–67.
20. Goedecke, K., Pignot, M., Goody, R. S., Scheidig, A. J., and Weinhold, E. (2001) Structure of the N6-adenine DNA methyltransferase M.TaqI in complex with DNA and a cofactor analog. *Nat. Struct. Biol. 8*, 121–125.
21. Lenz, T., Bonnist, E. Y., Pljevaljcic, G., Neely, R. K., Dryden, D. T., Scheidig, A. J., Jones, A. C., and Weinhold, E. (2007) 2-Aminopurine flipped into the active site of the adenine-specific DNA methyltransferase M.TaqI: Crystal structures and time-resolved fluorescence. *J. Am. Chem. Soc. 129*, 6240–6248.
22. Pljevaljcic, G., Schmidt, F., Scheidig, A. J., Lurz, R., and Weinhold, E. (2007) Quantitative labeling of long plasmid DNA with nanometer precision. *ChemBioChem 8*, 1516–1519.
23. Hawkey, P. M., and Jones, A. M. (2009) The changing epidemiology of resistance. *J. Antimicrob. Chemother. 64* (Suppl. 1), i3–i10.
24. Comartin, D. J., and Brown, E. D. (2006) Non-ribosomal factors in ribosome subunit assembly are emerging targets for new antibacterial drugs. *Curr. Opin. Pharmacol. 6*, 453–458.
25. Champney, W. S. (2006) The other target for ribosomal antibiotics: Inhibition of bacterial ribosomal subunit formation. *Infect. Disord. Drug Targets 6*, 377–390.
26. Poldermans, B., Roza, L., and Van Knippenberg, P. H. (1979) Studies on the function of two adjacent N6,N6-dimethyladenosines near the 3′ end of 16 S ribosomal RNA of *Escherichia coli*. III. Purification and properties of the methylating enzyme and methylase-30S interactions. *J. Biol. Chem. 254*, 9094–9100.
27. O'Farrell, H. C., Pulicherla, N., Desai, P. M., and Rife, J. P. (2006) Recognition of a complex substrate by the KsgA/Dim1 family of enzymes has been conserved throughout evolution. *RNA 12*, 725–733.
28. Adams, P. D., Grosse-Kunstleve, R. W., Hung, L. W., Ioerger, T. R., McCoy, A. J., Moriarty, N. W., Read, R. J., Sacchettini, J. C., Sauter, N. K., and Terwilliger, T. C. (2002) PHENIX: Building new software for automated crystallographic structure determination. *Acta Crystallogr. D58*, 1948–1954.
29. Emsley, P., and Cowtan, K. (2004) Coot: Model-building tools for molecular graphics. *Acta Crystallogr. D60*, 2126–2132.
30. Murshudov, G. N., Vagin, A. A., and Dodson, E. J. (1997) Refinement of macromolecular structures by the maximum-likelihood method. *Acta Crystallogr. D53*, 240–255.
31. DeLano, W. L. (2002) The PyMOL Molecular Graphics System, DeLano Scientific, Palo Alto, CA.
32. O'Farrell, H. C., Xu, Z., Culver, G. M., and Rife, J. P. (2008) Sequence and structural evolution of the KsgA/Dim1 methyltransferase family. *BMC Res. Notes 1*, 108.
33. Newby, Z. E., Lau, E. Y., and Bruice, T. C. (2002) A theoretical examination of the factors controlling the catalytic efficiency of the DNA-(adenine-N6)-methyltransferase from *Thermus aquaticus*. *Proc. Natl. Acad. Sci. U.S.A. 99*, 7922–7927.
34. Pues, H., Bleimling, N., Holz, B., Wolcke, J., and Weinhold, E. (1999) Functional roles of the conserved aromatic amino acid residues at position 108 (motif IV) and position 196 (motif VIII) in base flipping and catalysis by the N6-adenine DNA methyltransferase from *Thermus aquaticus*. *Biochemistry 38*, 1426–1434.
35. Maravic, G., Feder, M., Pongor, S., Flogel, M., and Bujnicki, J. M. (2003) Mutational analysis defines the roles of conserved amino acid residues in the predicted catalytic pocket of the rRNA:M6A methyltransferase ErmC′. *J. Mol. Biol. 332*, 99–109.
36. Schubert, H. L., Blumenthal, R. M., and Cheng, X. (2003) Many paths to methyltransfer: A chronicle of convergence. *Trends Biochem. Sci. 28*, 329–335.